The object of the study is the hydraulic braking system of heavy vehicles under conditions of progressive brake fluid leakage, with particular emphasis on its effect on braking performance and failure behavior. The problem addressed is the loss of braking performance due to hydraulic brake failure caused by fluid leakage, which reduces hydraulic pressure and may lead to total brake failure.

This study presents the design and experimental analysis of an independent mechanical wheel-clamp-based secondary safety brake for heavy vehicle braking systems. Experimental evaluation was conducted using a rotational test rig under varying load conditions. The results show that brake failure is strongly dependent on load. Under low load (5 Hz), total failure occurs at approximately 70 mL leakage and 5 bars, whereas under high load (50 Hz), failure occurs at only 25 mL and 9.3 bar, indicating increased sensitivity to leakage. This behavior is explained by the loss of hydraulic fluid and the compressibility of trapped air in the braking circuit, which prevents pressure from reaching its maximum level and reduces effective force transmission. Under total hydraulic failure, the secondary safety brake is capable of stopping wheel rotation across all tested conditions; however, the stopping time is longer, reaching up to 6.5 s compared to 1.4–2.9 s for the primary brake. These results demonstrate that the proposed system provides a fully independent fail-safe braking mechanism capable of maintaining braking functionality when the primary system fails, thereby addressing the problem of brake performance loss under hydraulic failure conditions. The system can be applied in heavy vehicle braking systems as a risk mitigation solution under failure scenarios, particularly in high-load operating conditions, with potential for further development, experimental refinement, and real vehicle implementation, including integration with activation strategies

Keywords: secondary safety brake, leakage, stopping time, pressure threshold, failure zone

UDC 629
DOI: 10.15587/1729-4061.2026.354678

IDENTIFICATION OF THE PERFORMANCE MECHANICAL SECONDARY SAFETY BRAKE UNDER HYDRAULIC FAILURE CONDITIONS: EXPERIMENTAL ASSESSMENT UNDER FLUID LEAKAGE

Rolan Siregar
Corresponding author
Doctor of Mechanical Engineering, Lecturer
Department of Mechanical Engineering*
E-mail: rolansiregar@ft.unsada.ac.id
ORCID: https://orcid.org/0000-0002-0300-7094
Asyari
Doctor of Mechanical Engineering, Lecturer
Department of Mechanical Engineering*
ORCID: https://orcid.org/0009-0003-4504-8083
Suzuki Syofian
Master of Information Engineering, Lecturer
Department of Information Engineering*
ORCID: https://orcid.org/0000-0003-3105-8259
*Darma Persada University
Taman Malaka Selatan str., 8, RT.8/RW.6,
Pd. Klp., Kec. Duren Sawit, Kota Jakarta Timur,
Daerah Khusus Ibukota, Jakarta, Indonesia, 134500

Received 18.03.2026
Received in revised form 03.04.2026
Accepted 15.04.2026
Published 30.04.2026

How to Cite: *Siregar, R., Asyari, Syofian, S. (2026). Identification of the performance mechanical secondary safety brake under hydraulic failure conditions: experimental assessment under fluid leakage. Eastern-European Journal of Enterprise Technologies, 2 (1 (140)), 57–65. https://doi.org/10.15587/1729-4061.2026.354678*

1. Introduction

The reliability of braking system is a fundamental requirement for ensuring vehicle safety, especially for heavy vehicles operating under high loads, steep road gradients [1, 2], and long travel distances; such conditions can lead to premature deterioration of braking performance. Numerous cases in Indonesia show that brake system failures occur frequently [3], particularly on heavy vehicles [4, 5], and often result in multi-vehicle collisions. Indonesia's geographic and tropical climate conditions, characterized by predominantly uphill and downhill roads, long travel distances, and high road-surface temperatures, intensify the loading on the braking system, accelerate component degradation, and therefore make brake failures on heavy vehicles [6] significantly more severe in terms of safety than those on light vehicles.

In the context of frequent brake failures in heavy vehicles, one of the main causes is the hydraulic brake system; therefore, the development of a secondary safety brake as a second-layer safety brake when the primary brake fails is of great importance. A reduction in pressure within the hydraulic braking system directly reduces the ability of the brake actuator to generate braking force, potentially leading to partial or total loss of braking function with very limited warning to the driver. Hydraulic brake system failure can be triggered by brake fluid leakage, ingress of air into the system, thermal mechanisms [7, 8] such

as vapor lock [9, 10] due to high brake fluid temperatures, or non-thermal mechanisms causing gradual pressure degradation within the hydraulic circuit. The resulting adverse effects on brake system functionality include reduced effective braking force, unstable braking response, and increased stopping time and distance.

Technology of a secondary safety braking system based on a mechanically actuated wheel-clamp offers a highly beneficial innovation for preventing accidents due to loss of vehicle control. This innovation is particularly crucial under conditions of primary (hydraulic) brake system failure, given Indonesia's operational challenges involving extreme road topography, such as steep gradients and long travel distances. Considering that accidents caused by brake failure in heavy vehicles continue to occur and pose a persistent threat to public transport safety, the development of secondary braking systems for hydraulic failure conditions remains highly relevant in modern transportation systems.

2. Literary review and statement of the problem

Previous studies have focused on the performance of the primary braking system, particularly in terms of thermal behavior, material degradation, and braking efficiency. The paper [11] presents the fading behavior and wear mechanisms of a C/C–SiC brake disc during cyclic braking, the paper [12] analyzes the fade behavior of copper-based brake pads during emergency braking cycles at high speed and overload, and the paper [13] investigates the impact of initial braking temperature on thermal-induced brake fade during long downhill operation, showing that a higher initial temperature significantly increases the risk of coefficient-of-friction reduction and overall braking performance deterioration. These studies show that braking performance is strongly affected by temperature and material properties. However, these works mainly focus on improving the performance of primary brake components and do not address how braking capability can be maintained when the primary braking system fails.

Studies [14–16] examine brake cooling systems as a preventive approach to mitigate temperature rise. The paper [14] develops a coupled CFD-thermal simulation to predict vehicle brake cooling performance, showing that channel design and airflow configuration can significantly reduce the operating temperature of brake components. The study [15] designs and optimizes a forced-air cooling system for commercial vehicle brakes, resulting in a reduction of the maximum component temperature and improved cooling performance. The paper [16] analyzes the disc brake temperature distribution under convective cooling during repetitive braking, showing that the convective mode significantly affects the temperature pattern on the disc. Such preventive cooling-based approaches are effective in reducing thermal loading on the brake system, but they do not directly address hydraulic braking system failures caused by fluid leakage. One way to address this condition is the use of an additional brake or a mechanical brake that operates independently of the primary hydraulic system.

The papers [17, 18] investigate brake fluid formulation as a key element of the braking system. The study [17] uses R&D databases to develop a mixture-based design methodology for brake fluid formulations, enabling the creation of formulations that meet technical standards and market requirements, while accelerating product development and reducing the number of required experiments. The paper [18] proposes polyethylene glycol monomethyl ethers as the main component in brake fluid formulations, analyzing their physicochemical properties and feasibility in DOT-5.1-type brake fluids, including their influence on quality indices such as wet boiling point and performance over a wide temperature range. Although such formulation developments improve the thermal and chemical properties of brake fluid, early detection of micro-leakage in the hydraulic braking system remains a challenge, largely influenced by limitations in material compatibility, long-term formulation stability, and performance under various thermal and mechanical conditions.

The paper [19] explores the effects of emergency braking without an anti-lock braking system (ABS) on vehicle dynamics, demonstrating wheel lock-up on wet surfaces and providing important insight into the risk of loss of control during emergency braking without a skid-control system. The paper [20] develops an automatic emergency braking (AEB) control method oriented toward ride comfort, using a smoother deceleration strategy without sacrificing safety. AEB-based approaches are now widely implemented in modern vehicles, but they generally still rely on the primary hydraulic braking system as the actuator, so the AEB role is mainly focused on collision prevention under normal operating conditions rather than serving as a substitute for the primary hydraulic brake in the event of total failure. The study in [21] develops a secondary braking system tested on a rig for light vehicle wheels, demonstrating feasibility at a small scale. However, it does not address implementation in heavy vehicles, where higher loads and braking demands require different design considerations. In contrast, the study in [22] focuses on wheel chocks as an auxiliary safety mechanism, but it lacks a mechanical actuator structure, making it incapable of functioning as an active braking system. As a result, it cannot provide a dynamic or automated response during brake failure. Therefore, these studies leave a critical gap in the development of an actuated secondary braking system for heavy vehicles, which remains an important aspect in improving vehicle braking system performance and safety.

Overall, the reviewed literature shows that research on the development of an independent secondary safety braking system based on a mechanical wheel-clamp for conditions involving primary hydraulic brake system failure is highly important, given that primary brake failure cannot be entirely avoided. This highlights the need for a secondary safety braking strategy when the hydraulic braking system experiences disturbance or failure, for example by implementing an additional brake or a mechanical braking mechanism that does not depend on the integrity of the primary hydraulic circuit.

There is still limited understanding of the performance of an independent mechanical wheel-clamp-based secondary safety brake when the primary hydraulic braking system experiences disturbance or failure, particularly under high rotational energy conditions relevant to heavy vehicle operation. This limitation indicates the need for further investigation under controlled experimental conditions representative of heavy vehicle operation.

3. The aim and objectives of the study

The aim of the study is to identifying the performance of an independent mechanical wheel-clamp-based secondary safety brake when the primary hydraulic braking system experiences disturbance or failure, particularly under high

rotational energy conditions relevant to heavy vehicle operation. This will allow a better understanding of its braking capability and support its potential application as a safety backup under hydraulic failure conditions.

To achieve this aim, the following objectives are defined:

– to quantify the relationship between brake fluid leakage and hydraulic pressure under varying load conditions;

– to determine the hydraulic failure threshold and define activation criteria for the secondary braking system;

– to experimentally evaluate the braking performance of the secondary system under total hydraulic failure conditions;

– to compare the braking effectiveness between primary hydraulic and secondary braking systems.

4. Materials and methods

4. 1. The object and hypothesis of the study

The object of the study is the hydraulic braking system of heavy vehicles under conditions of progressive brake fluid leakage, with particular emphasis on its effect on braking performance and failure behavior.

The main hypothesis of the study is that progressive brake fluid leakage reduces hydraulic pressure in the braking circuit, leading to a degradation of braking performance, and that an actuated secondary safety brake can provide sufficient braking force under hydraulic failure conditions. The study assumes that the rotational test rig adequately represents the braking characteristics of heavy vehicles, particularly in terms of rotational energy and load conditions, and that brake fluid leakage occurs progressively, resulting in a corresponding reduction in hydraulic pressure. The study is conducted under controlled laboratory conditions and does not account for all real-world operating factors such as road surface variations, environmental conditions, and driver behavior, with the braking system evaluated under predefined operating scenarios to isolate the effects of hydraulic failure and secondary brake activation.

4. 2. Rotational test-rig configuration

The experiments were conducted using a rotational brake test rig [23, 24] designed to evaluate hydraulic brake failure and the performance of a secondary safety brake at the subsystem level. This test rig enables the analysis of wheel rotational dynamics independently of vehicle translational motion. The main components of the test rig consist of:

1) an electric drive motor controlled;
2) a variable frequency drive (VFD);
3) a heavy-vehicle wheel;
4) a primary hydraulic braking system;
5) a mechanically independent secondary safety brake;
6) a monitoring, control, and data acquisition system;
7) a valve;
8) a measuring cup;
9) a pressure transmitter (Fig. 1).

The wheel rotational speed was controlled by an electric motor operated below its base frequency to ensure stable torque characteristics. The actual wheel speed was measured using a non-contact infrared tachometer with a reflective marker attached to the wheel surface. The primary hydraulic braking system and the secondary safety brake act directly on the wheel assemblies mounted on a single axle, enabling direct observation of braking response at the axle level without being influenced by vehicle-level dynamics. Similar rotational [25] and inertia-based brake test rigs have been widely employed to characterize braking behavior at the subsystem level while eliminating the effects of full-vehicle dynamics. Baseline braking tests were first conducted under normal hydraulic operating conditions to establish reproducible initial rotational states and to characterize stopping time and rotational kinetic energy dissipation. In each test, the axle was accelerated to a target rotational speed and maintained under steady-state conditions before braking was applied. The stopping time, defined as the time interval between the application of the braking force and the complete cessation of axle rotation, was recorded. Each test condition was repeated multiple times to ensure the reproducibility of the measurement results. For energy-based analysis, the rotating system was represented using an equivalent rotational inertia at the shaft level. The rotational inertia of a single wheel-tire assembly was estimated as $I_\omega = 6.75\ \text{kg} \cdot \text{m}^2$. Because two identical wheel-tire assemblies rotate synchronously on the test axle, the equivalent rotational inertia at the axle level is approximated as

$$I_{axle} \approx 2I_\omega.$$

Any additional inertia from the drivetrain system is neglected in this first-order approximation. Although this assumption affects the absolute values of the reported rotational energy and braking power, it does not alter the observed trends, stopping behavior, or the identified hydraulic failure thresholds.

a *b*

Fig. 1. Rotational brake test rig:
a — subsystem configuration for evaluating hydraulic brake failure and secondary safety brake performance; *b* — leakage process mechanism

4. 3. Hydraulic brake failure induced by controlled fluid leakage

Hydraulic brake failure was generated experimentally through controlled leakage of brake fluid using a valve installed on the brake hose. The valve was integrated into the brake line to enable a gradual and quantifiable reduction in brake fluid volume. The fluid was released in fixed increments of 5 mL at each stage. After each leakage stage, the system was deliberately not subjected to a bleeding process, thereby allowing air to remain trapped within the hydraulic brake line.

Brake line pressure was continuously monitored using a pressure transmitter installed in the hydraulic brake hose. At each leakage level and wheel rotational speed, the braking response was evaluated by applying the primary brake under steady-state axle rotational conditions. Based on the measured

pressure and the observed braking effectiveness, the system behavior was classified into three operating conditions, in addition to normal braking: incipient brake malfunction, brake malfunction, and total hydraulic failure. Incipient brake malfunction was defined as the initial onset of braking degradation from normal operation. Brake malfunction was identified when wheel rotation could still be decelerated but could not be brought to a complete stop. Total hydraulic failure was defined as a condition in which the brake produced no observable effect on axle rotation.

4. 4. Activation of the secondary safety brake

The performance evaluation of the secondary safety brake was conducted under total hydraulic failure conditions. The secondary brake was activated manually using an emergency switch to ensure precise timing and test repeatability, while isolating subsystem performance from detection and control delays associated with automatic activation. For each test condition, the wheel was first stabilized at the target rotational speed before the secondary safety brake was engaged. The stopping time was recorded to assess braking capability, operational limits, and the performance consistency of the secondary safety brake.

5. Results of the study on hydraulic brake failure and secondary safety brake performance

5. 1. Effect of brake fluid leakage on hydraulic pressure under varying load conditions

Baseline tests were performed to establish stable and consistent reference conditions, which serve as a benchmark for failure evaluation and emergency braking system analysis. The main characteristics of the hydraulic braking system in the test rig include inertial load, energy, braking power, and stopping time. These characteristics are evaluated under normal operating conditions as a baseline for analyzing brake system failures caused by brake fluid leakage and the use of a secondary braking system under emergency conditions. The baseline rotational braking characteristics obtained under normal hydraulic operating conditions are summarized in Table 1.

Table 1

Baseline rotational braking characteristics under normal hydraulic operation (axle-level values)

Motor frequency (Hz)	Wheel speed (rpm)	Axle-level inertia I_{axle} (kg · m^2)	Axle-level energy $E_{rot,axle}$ (J)	Stopping time t (s)	Average braking power $P_{EK,axle}$ (W)
10	99	13.50	726	1.40	518
20	202	13.50	3,018	2.00	1,51
30	299	13.50	6,614	2.10	3,15
40	399	13.50	11,778	2.50	4,712
50	499	13.50	18,422	2.90	6,352

Note: Axle-level rotational kinetic energy and braking power are calculated assuming two identical wheel-tire assemblies rotating synchronously on a single axle.

Because the measured stopping response reflects the combined braking action of two brake units acting on a single axle, the reported rotational kinetic energy and average braking power are expressed at the axle level. Under normal hydraulic operating conditions, the rotational brake test rig exhibited consistent braking behavior across the tested frequency range. As shown in Table 1, rotational energy and braking power increase with increasing motor frequency, while the stopping time varies within the range of 1.4–2.9 s.

Hydraulic brake failure was modeled through gradual brake fluid leakage without a bleeding process, resulting in progressive pressure degradation under each variation of braking load. Braking performance characteristics under failure conditions caused by brake fluid leakage are reflected in the generated brake pressure and the capability of the hydraulic braking system to sustain the load, as presented in Table 2.

Table 2

Hydraulic brake leakage test results and failure classification, showing that increasing leakage reduces brake pressure and accelerates failure, particularly at higher load levels

Leak step (mL)	Total leakage (mL)	5 Hz (P/S)	10 Hz (P/S)	15 Hz (P/S)	20 Hz (P/S)	25 Hz (P/S)	30 Hz (P/S)	35 Hz (P/S)	40 Hz (P/S)	45 Hz (P/S)	50 Hz (P/S)
0	0	11/N	11/N	11/N	11/N	11/N	11/N	11/N	11/N	11/N	11/N
5	5	11/N	11/N	11/N	11/N	11/N	11/N	11/N	11/N	11/N	11/N
5	10	11/N	10.5/N	11/N	10/N	10.5/N	10.5/N	10.5/N	10.5/N	10.5/N	10.5/N
5	15	10/N	10/N	10.5/N	9.5/N	10/N	10/N	10/I	10/I	10.3/I	10.3/I
5	20	10/N	10/N	9/N	9/N	9.5/I	9.5/I	9.5/M	9.5/M	10/M	10/M
5	25	9.5/N	9.5/N	9/N	9.3/I	9/M	9/M	9/M	9/M	9/F	9.3/F
5	30	9.5/N	9.5/N	9/N	9/M	8.5/M	8.5/M	9/M	8.7/F	–	–
5	35	9/N	9.5/N	9/I	9/M	8.5/M	8.5/F	8.7/F	–	–	–
5	40	9/N	9/N	8.7/M	8.5/M	8.3/M	–	–	–	–	–
5	45	8/N	8.5/I	8.7/M	8.5/M	8/F	–	–	–	–	–
5	50	8/N	8.5/M	8.5/M	8.3/M	–	–	–	–	–	–
5	55	7.5/I	7.5/M	8/M	8/F	–	–	–	–	–	–
5	60	7/M	7/M	7/F	–	–	–	–	–	–	–
5	65	6/M	6.5/F	–	–	–	–	–	–	–	–
5	70	5/F	–	–	–	–	–	–	–	–	–

Note: P – brake pressure (bar); S – brake performance status. Status codes: N – normal operation; I – indication of malfunction; M – brake malfunction; F – total brake failure; "–" – test not conducted due to prior total brake failure.

Table 1 presents the operating conditions of the hydraulic braking system under measured brake fluid leakage, where braking conditions are categorized for each load variation through changes in rotational energy controlled by an electric motor inverter (variable frequency drive, VFD). The observed phenomena describe the relationship between brake pressure and braking conditions, classified as normal (N), initial indication of malfunction (I), brake malfunction (M), and total brake failure (F). A normal condition (N) is defined when the braking system is able to stop the wheel rotation. The initial malfunction indication (I) is defined when the wheel rotation can barely be stopped or when an unusually long delay occurs before the wheel comes to a stop. Brake malfunction (M) is defined when the wheel cannot be completely stopped but its rotational speed can still be reduced. Meanwhile, total brake failure (F) indicates that the brake no longer has any effect in slowing down the wheel rotation, meaning that the braking system has completely lost its effectiveness.

To identify brake failure due to the effect of fluid leakage under each loading variation, the results can be presented in graphical form as shown in Fig. 2.

Based on the graph in Fig. 2, it can be explained that starting from a low load (frequency of 5 Hz), total brake failure occurs only after the total fluid leakage reaches 70 mL. Meanwhile, at a higher load, such as at a frequency of 50 Hz, a fluid loss of only 25 mL is sufficient to cause brake failure. The results show that total brake failure occurs at different leakage volumes depending on the load level. At 5 Hz, failure occurs at 70 mL, whereas at 50 Hz, failure occurs at 25 mL. Therefore, the operational duration of the braking system becomes shorter as the braking load increases when brake fluid leakage occurs.

Furthermore, total brake failure due to fluid leakage at low frequency, such as 5 Hz, begins to occur at a brake pressure of 5 bar. This failure becomes more likely as the load increases. At higher frequencies, such as 50 Hz, failure already occurs at a brake pressure of 9.3 bar. Total brake failure occurs at 5 bar under 5 Hz and at 9.3 bar under 50 Hz.

5. 2. Hydraulic failure threshold and secondary brake activation conditions

As a visual representation of the experimental results, Fig. 3 presents a hydraulic failure threshold map that illustrates the operational limits of the braking system. This map shows the influence of rotational energy, represented by the VFD frequency, as well as the volume of fluid leakage on brake failure conditions.

The graph shows the condition of the braking system under variations in frequency and fluid loss volume in the form of operational zones. It can be observed that at low frequencies, the safe operating region remains wide, whereas at higher frequencies, the failure region expands even at relatively small fluid loss volumes. The transition boundary between safe, malfunction, and total failure conditions becomes increasingly narrow as the frequency increases. The transition boundary between normal, malfunction, and failure conditions shifts toward lower leakage volumes as the frequency increases. Conditions corresponding to total hydraulic failure were used as the basis for defining the activation threshold of the secondary safety brake system. It should be noted that these conditions were applied in test rig experiments, whereas in actual vehicle operation, activation can be implemented more flexibly as needed, including from the early indication of malfunction.

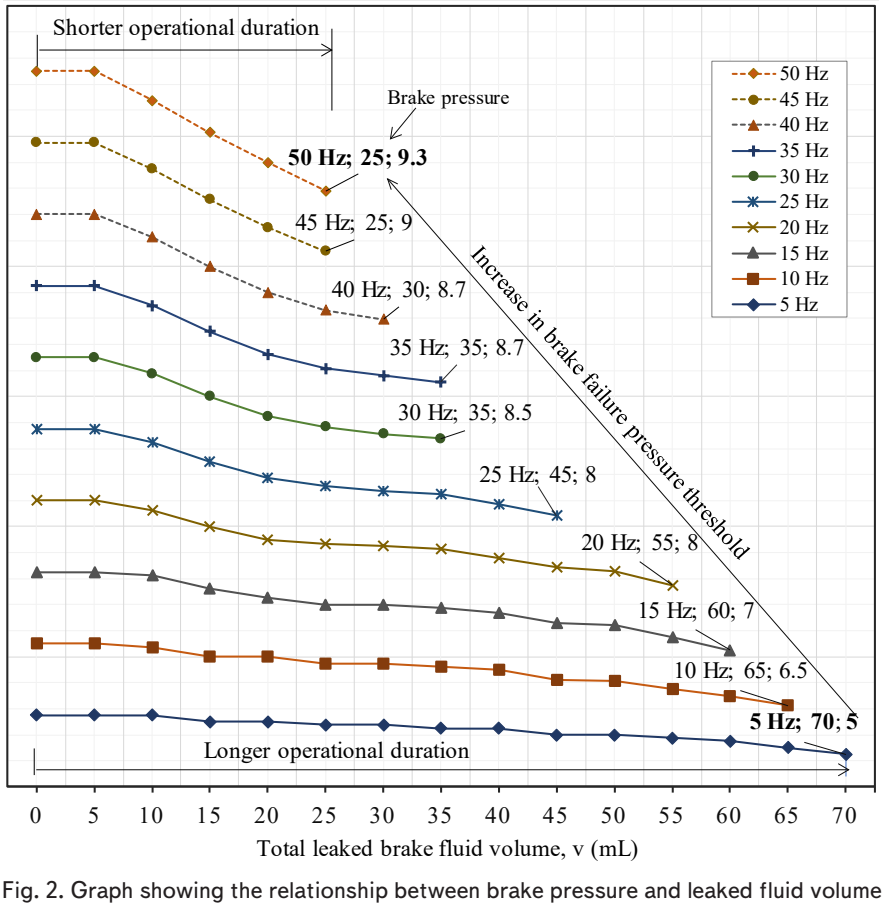

Fig. 2. Graph showing the relationship between brake pressure and leaked fluid volume at different load levels (VFD frequencies) during rig testing

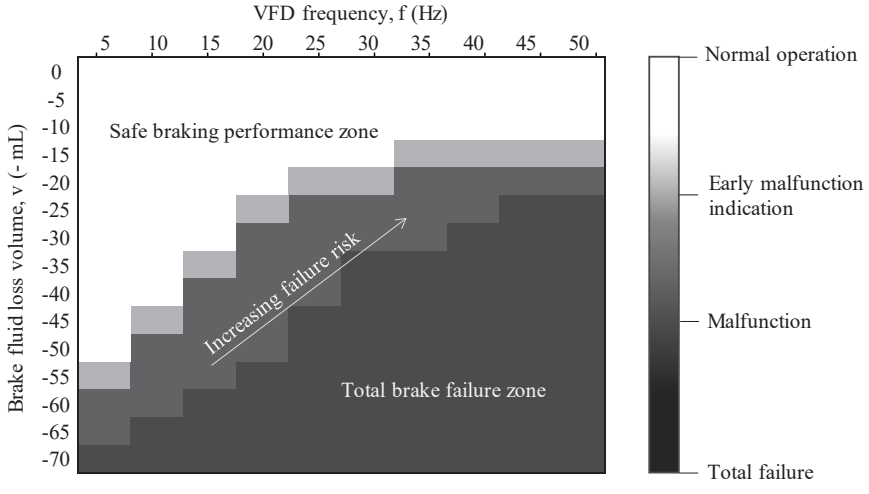

Fig. 3. Hydraulic failure map indicating the operational limits of the braking system, showing the transition from safe operation to malfunction and failure as leakage and load increase

5. 3. Performance of the secondary safety brake under total hydraulic failure conditions

The braking response following total hydraulic failure is illustrated in Fig. 4, which compares the stopping times achieved by the secondary safety brake with those obtained under normal hydraulic braking across the entire tested frequency range, thereby highlighting the performance gap between the primary and secondary braking systems.

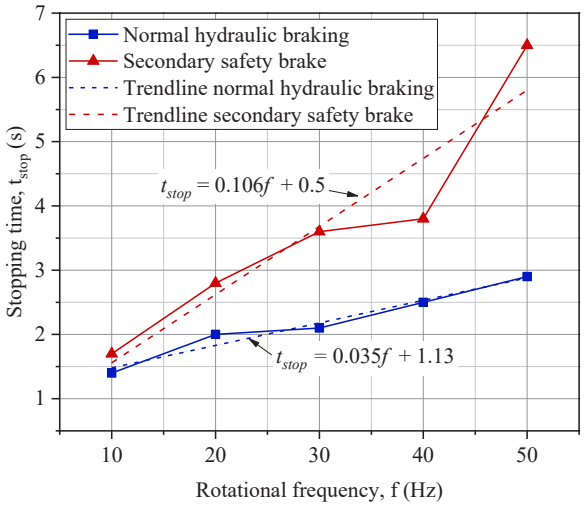

Fig. 4. Comparison of axle stopping times under normal hydraulic braking and secondary safety brake activation

The comparison of wheel stopping time between normal hydraulic braking and the secondary safety brake shows a significant difference. The stopping time achieved by the hydraulic brake (primary brake) is consistently shorter than that of the secondary safety brake. This is indicated by the trendline slope of normal hydraulic braking, which is less steep than that of the secondary safety brake, as shown in Fig. 4.

The stopping time of the secondary safety brake is consistently longer than that of the primary hydraulic brake across all tested conditions. At low load conditions, both systems exhibit relatively similar stopping times, with 1.4 s for the hydraulic brake and 1.7 s for the secondary safety brake. However, as the load increases, the difference in stopping time follows an approximately linear trend with a relatively large difference in gradient. At the maximum load tested, the stopping time (t_{stop}) for the hydraulic brake is 2.9 s, whereas for the secondary safety brake it reaches 6.5 s. Nevertheless, the secondary safety brake is capable of stopping wheel rotation across all tested load conditions.

5. 4. Comparison of braking effectiveness between primary and secondary braking systems

All energy and braking power values are expressed at the axle level, consistent with the two-brake-unit configuration on a single axle and the measured stopping response. To provide a more fundamental interpretation, the braking behavior was analyzed based on the relationship between the initial rotational kinetic energy and the net braking power, as shown in Fig. 5.

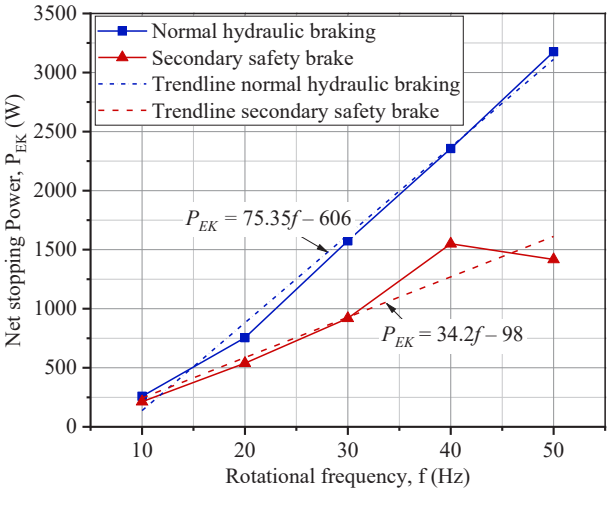

Fig. 5. Energy-based interpretation of secondary safety brake performance

Fig. 5 shows that the primary hydraulic braking system is able to increase braking power proportionally and linearly with increasing rotational energy, producing higher values than the secondary safety brake. Although both systems exhibit relatively similar performance at low energy levels, at higher energy levels the braking power of the secondary safety brake increases more slowly and tends to decrease relative to the primary system.

The results show that braking power of the primary system increases proportionally with rotational energy, while the secondary system exhibits a lower rate of increase at higher energy levels. The energy-based comparison provides a basis for evaluating the performance characteristics of both braking systems.

6. Discussion on brake failure characteristics and secondary safety brake performance

The experimental results reveal the progressive failure characteristics of the braking system caused by hydraulic fluid leakage. Under low load conditions, leakage does not immediately lead to noticeable performance degradation, as the braking system is still capable of absorbing the rotational energy of the wheel. Degradation becomes evident only after a significant reduction in fluid volume, as observed in Fig. 2 at low frequencies (e.g., 5 Hz). In contrast, under high braking loads, the system becomes highly sensitive to leakage, and even small fluid losses can rapidly trigger brake failure, as shown at higher frequencies (e.g., 50 Hz). These findings indicate that minor damage, such as fluid leakage, may not produce observable symptoms under light operating conditions, but can lead to critical failure under high load conditions (Fig. 3). This behavior is particularly hazardous in real-world scenarios, such as downhill driving, where the braking system operates near its maximum capacity and the risk of failure is significantly increased.

The performance characteristics of the secondary safety brake under total hydraulic failure conditions are further illustrated in Fig. 4, 5. As shown in Fig. 4, the stopping time of the secondary safety brake is consistently longer than that of the primary hydraulic braking system across all tested rotational frequencies. While both systems exhibit comparable performance at low rotational energy levels, the difference becomes more pronounced as the load increases, indicating a lower braking efficiency of the secondary system under high-energy conditions. This trend is further supported by the energy-based analysis presented in Fig. 5, where the braking power of the secondary safety brake increases at a lower rate compared to the primary system. At higher rotational energy levels, the secondary system shows a tendency toward reduced effectiveness relative to the hydraulic brake. Nevertheless, the ability of the secondary system to consistently stop wheel rotation under all tested conditions confirms its functional reliability as a fail-safe mechanism.

A systematic comparison with previous studies highlights key differences in system design, activation mechanism, level of independence, and failure-handling capability. Study [21] developed a secondary braking system for light vehicles at the test rig level; however, it remains limited in energy capacity and relies on driver-induced pedal pressure for activation, introducing uncertainty in activation thresholds. Study [26] investigated adaptive brake control for a secondary braking system in multi-axle vehicles. Although it improves control performance, the secondary function remains integrated with the primary system, introducing the risk of simultaneous failure. In contrast, the present study proposes a secondary safety brake that is fully independent of the primary hydraulic circuit, both in terms of actuation and braking force generation. The system is specifically designed for heavy vehicle conditions, considering the high rotational energy involved. Experimental results demonstrate that the system remains functional under total hydraulic failure conditions, even when the primary brake is unable to generate any effective braking force. Moreover, the system is capable of stopping wheel rotation across the entire range of tested loads, although with longer stopping times compared to the primary braking system.

Therefore, the scientific problem related to the absence of an independent fail-safe mechanism under total hydraulic brake failure can be considered addressed at the system level. Unlike previous approaches that retain dependency on the primary braking system, the proposed method provides an additional, fully independent safety layer capable of operating under complete system failure. However, given the complexity of brake malfunction phenomena, the proposed system should be regarded as a risk mitigation strategy rather than a replacement for the primary braking system.

Despite these findings, several limitations of the present study should be acknowledged. The proposed framework is based on a subsystem level evaluation using a rotational test rig and does not directly represent translational braking performance at the full vehicle level. By excluding vehicle-level effects such as tire–road interaction and suspension dynamics, the study enables controlled identification of hydraulic failure thresholds and characterization of fail safe braking behavior; however, these simplifications limit direct applicability to real world driving conditions. Furthermore, automatic activation strategies and control logic for the secondary safety brake were not considered and remain subjects for future research. Overall, the findings demonstrate the feasibility of an independent secondary safety braking system as a fail-safe mechanism, while highlighting the need for further development toward real vehicle implementation.

7. Conclusions

1. The relationship between brake fluid leakage and hydraulic pressure shows that increasing leakage leads to progressive pressure degradation under all load conditions. However, the effect becomes more critical at higher loads, where smaller leakage volumes result in significant reductions in braking performance. This is seen when total brake failure occurs at a leakage volume of approximately 70 mL under low load conditions (5 Hz), whereas at high load conditions (50 Hz), failure occurs at only 25 mL. In addition, the corresponding failure pressure increases from approximately 5 bar at 5 Hz to about 9.3 bar at 50 Hz, indicating a higher sensitivity of the braking system to leakage under increased load conditions.

2. The hydraulic failure threshold is strongly influenced by load conditions. Under low load (5 Hz), total brake failure occurs at approximately 70 mL of fluid leakage and 5 bar, whereas under high load (50 Hz), failure occurs at approximately 25 mL and 9.3 bar, indicating that higher loads significantly reduce the system's tolerance to leakage and define the activation condition for the secondary safety brake.

3. The experimental evaluation of the secondary safety brake under total hydraulic failure shows that the system is capable of stopping wheel rotation across all tested load conditions. However, the stopping time is longer compared to normal hydraulic braking, reaching up to 6.5 s at maximum load.

4. The comparison between the primary hydraulic brake and the secondary safety brake demonstrates that the primary system provides higher braking performance, with shorter stopping times (1.4–2.9 s) and greater braking power. In contrast, the secondary system exhibits lower braking effectiveness at

higher energy levels, but remains functional as an independent fail-safe mechanism under total hydraulic failure conditions.

Conflict of interest

The authors declare that they have no conflict of interest in relation to this study, whether financial, personal, authorship or otherwise, that could affect the study and its results presented in this paper.

Financing

The development of the secondary safety brake model through test rig testing was funded by the Directorate of Research and Community Service (DPPM) Kemdiktisaintek of Indonesia under the 2025 fiscal year research grant program, applied research scheme with model output (PTLM).

Data availability

Data will be made available on reasonable request.

Use of artificial intelligence

The authors confirm that they did not use artificial intelligence technologies in creating the submitted work.

Authors' contributions

Rolan Siregar: Conceptualization, Writing-original draft, Methodology, Data Curation, Writing – review & editing, Supervision; **Asyari**: Project administration; Resources, Formal analysis, Validation; **Suzuki Syofian**: Investigation, Project administration, Formal analysis, Supervision.

References

1. Wang, Z., Yu, Q., Han, F., Shi, P. (2016). Research on a Brake Temperature Model of Heavy-Duty Trucks Braking on Long Downhill. Journal of Highway and Transportation Research and Development (English Edition), 10 (3), 90–96. https://doi.org/10.1061/jhtrcq.0000524
2. Gang, W., Tian, C., ZhiPeng, L. (2023). Study on the influence of running parameters on the temperature field of disc brake on long downhill road. Proceedings of the Institution of Mechanical Engineers, Part D: Journal of Automobile Engineering, 238 (10-11), 3386–3398. https://doi.org/10.1177/09544070231177176
3. Budhi, W. S., Utanaka, A., Wiryasuta, I. K. H., Widyastuti, H. (2024). Identifying Traffic Accident Trends and Black Spot Locations on National Road (A Case Study: Rogojampi-Kabat, Banyuwangi). Advances in Civil Engineering Materials, 683–695. https://doi.org/10.1007/978-981-97-0751-5_60
4. Lu, Y., Wang, F., Zhang, G. (2020). Research on Brake Failure Control of Heavy Commercial Vehicles Based on Turning Conditions. 2020 4th CAA International Conference on Vehicular Control and Intelligence (CVCI), 395–400. https://doi.org/10.1109/cvci51460.2020.9338601
5. Haq, M. T., Ampadu, V.-M. K., Ksaibati, K. (2023). An investigation of brake failure related crashes and injury severity on mountainous roadways in Wyoming. Journal of Safety Research, 84, 7–17. https://doi.org/10.1016/j.jsr.2022.10.003
6. Wang, F., Lu, Y., Li, H. (2022). Heavy-Duty Vehicle Braking Stability Control and HIL Verification for Improving Traffic Safety. Journal of Advanced Transportation, 2022, 1–27. https://doi.org/10.1155/2022/5680599
7. Umaras, E., Barari, A., Tsuzuki, M. S. G. (2021). Heavy Vehicles Brake Drums – An Accurate Evaluation on Thermal Loads in Severe Service Conditions. International Journal of Automotive Technology, 22 (2), 371–382. https://doi.org/10.1007/s12239-021-0035-1
8. Kosbe, P., Patil, P., Kulkarni, R. (2020). Fade and recovery characteristics of commercial disc brake friction materials: a case study. International Journal of Ambient Energy, 43 (1), 2446–2452. https://doi.org/10.1080/01430750.2020.1730959
9. Hilden, M., Dietl, H. (2024). Improvements in brake fluid standardization to avoid noise & wear. 14th International Munich Chassis Symposium 2023, 425–437. https://doi.org/10.1007/978-3-662-70348-9_26
10. Kawakami, A., Shikada, A., Miyao, K. (2000). Control method for brake vapor lock in automobiles. JSAE Review, 21 (1), 73–78. https://doi.org/10.1016/s0389-4304(99)00066-1
11. Hui, Y., Liu, G., Zhang, Q., Zhang, Y., Zang, Y., Wang, S., Shi, R. (2023). Fading behavior and wear mechanisms of C/C–SiC brake disc during cyclic braking. Wear, 526-527, 204930. https://doi.org/10.1016/j.wear.2023.204930
12. Zhang, P., Zhang, L., Fu, K., Wu, P., Cao, J., Shijia, C., Qu, X. (2019). Fade behaviour of copper-based brake pad during cyclic emergency braking at high speed and overload condition. Wear, 428-429, 10–23. https://doi.org/10.1016/j.wear.2019.01.126
13. Zhang, Q., Liu, H., He, Z., Mo, J., Jin, W., Shen, M., Zhao, C. (2025). Impact of initial braking temperature on thermal-induced brake fade during long-downhill operations. Engineering Failure Analysis, 167, 109077. https://doi.org/10.1016/j.engfailanal.2024.109077
14. Vdovin, A., Gustafsson, M., Sebben, S. (2018). A coupled approach for vehicle brake cooling performance simulations. International Journal of Thermal Sciences, 132, 257–266. https://doi.org/10.1016/j.ijthermalsci.2018.05.016
15. Peng, D., Tan, G., Tang, J., Guo, X. (2021). Design and Optimization of Forced-Air Cooling System for Commercial Vehicle Brake System. SAE International Journal of Commercial Vehicles, 15 (1), 15–25. https://doi.org/10.4271/02-14-04-0031
16. Adamowicz, A., Grzes, P. (2011). Influence of convective cooling on a disc brake temperature distribution during repetitive braking. Applied Thermal Engineering, 31 (14-15), 2177–2185. https://doi.org/10.1016/j.applthermaleng.2011.05.016
17. de Freitas, L. H., Roux, G. A. C. L. (2009). Exploiting R&D Databases for Efficient Product Design: Application to Brake Fluid Formulations. 10th International Symposium on Process Systems Engineering: Part A, 1161–1166. https://doi.org/10.1016/s1570-7946(09)70414-6

18. Khamidullin, R. F., Bashkirtseva, N. Yu., Abdullin, A. I., Akhmetov, I. I. (2006). Polyethylene glycol monomethyl ethers as the main component of brake fluid. Russian Journal of Applied Chemistry, 79 (11), 1853–1856. https://doi.org/10.1134/s107042720611022x
19. Zulhilmi, I. M., Peeie, M. H., Asyraf, S. M., Sollehudin, I. M., Ishak, I. M. (2020). Experimental Study on the Effect of Emergency Braking without Anti-Lock Braking System to Vehicle Dynamics Behaviour. International Journal of Automotive and Mechanical Engineering, 17 (2), 7832–7841. https://doi.org/10.15282/ijame.17.2.2020.02.0583
20. Lai, F., Liu, J., Hu, Y. (2024). An Automatic Emergency Braking Control Method for Improving Ride Comfort. World Electric Vehicle Journal, 15 (6), 259. https://doi.org/10.3390/wevj15060259
21. Kurhade, A. S., Tiwari, A. P., Wadkar, R. M., Kumar, S. (2017). Development of Secondary Braking System in Order Reduce Accidents Happening Due to Brake Failure. IJSRD – International Journal for Scientific Research & Development, 5 (10), 584–586. Available at: https://www.ijsrd.com/articles/IJSRDV5I100332.pdf
22. Rancourt, D., Khazoom, C., Blanchette, C., Giraud, L., Lemire, J., St-Amant, Y. (2018). Wheel Chock Key Design Elements and Geometrical Profile for Truck Vehicle Restraint. SAE International Journal of Transportation Safety, 06 (1), 69–84. https://doi.org/10.4271/09-06-01-0006
23. Adhitya, M., Siregar, R., Sumarsono, D. A., Nazaruddin, N., Heryana, G., Prasetyo, S., Zainuri, F. (2020). Experimental analysis in the test rig to detect temperature at the surface disc brake rotor using rubbing thermocouple. Eastern-European Journal of Enterprise Technologies, 2 (5 (104)), 6–11. https://doi.org/10.15587/1729-4061.2020.191949
24. Limpert, R. (2011). Brake Design and Safety, Third Edition R-398. SAE International. https://doi.org/10.4271/r-398
25. Siregar, R., Adhitya, M., Sumarsono, D. A., Nazaruddin, N., Heryana, G., Prasetya, S., Zainuri, F. (2021). Optimization of temperature measurement on the bus drum brake as a basis for developing brake fault signals. Eastern-European Journal of Enterprise Technologies, 1 (1 (109)), 13–19. https://doi.org/10.15587/1729-4061.2021.224907
26. Bogomolov, V., Klimenko, V., Leontiev, D., Kuripka, O., Frolov, A., Don, Y. (2021). Features of adaptive brake control of the secondary brake system of a multi-axle vehicle. Automobile Transport, 48, 27–37. https://doi.org/10.30977/at.2219-8342.2021.48.0.27